WOOD RESEARCH
56 (2): 2011
221-232

FT-IR AND TGA STUDIES ON LIQUFIED WOOD PRODUCTS IN THE CONDENSATION REACTION PROCESS

Min Niu, Guangjie Zhao
Beijing Forestry University, College of Materials Science and Technology
Haidian, Beijing, China

Mehmet Hakki Alma
Kahramanmaras Sutcu Imam University, Faculty of Forestry
Kahramanmaras, Turkey

(Received November 2010)

ABSTRACT

To provide some basic information to the research of condensation reaction mechanism in the last stage of wood liquefaction, the chemical groups and weight loss behaviors in pyrolysis were investigated by using Fourier transform infrared spectroscopic (FT-IR) and thermogravimetric analysis (TGA) in this study. The results showed that the liquefaction time had an important effect on the chemical groups of liquefied wood products. With the prolongation of the liquefaction time, the absorbance intensity of the peaks from cellulose at 1709 cm^{-1} and lignin at 1648, 1357 and 1243 cm^{-1} increased gradually. Compared with wood itself and decomposition products, condensation products had higher weight loss percents and lower residual ratios. In other word, the thermal stabilities of condensation products decreased in TGA pyrolysis. And the values of the apparent activation energy descended. Furthermore, the reaction order values of all the samples were less than 1, as suggested that the liquefaction time had smaller influences on pyrolysis mechanism.

KEYWORDS: Wood liquefaction, *Betula dahurica* Pall, Fourier transform infrared spectroscopic (FT-IR), thermogravimetric analysis (TG), decomposition products, condensation products.

INTRODUCTION

Many researchers have used biomass materials to substitute for fossil recourses and to prepare biomass products successfully in the presence of polyhydric alcohols/phenol and acid catalysts (Kunaver et al. 2010, Chen and Lu 2009, Ahmadzadeh and Zakaria 2009). However,

the liquefaction residual yield resulted from condensation reaction in last stage of lignocellulosic liquefaction was higher when less liquefying reagents were added into the liquefaction system. As not only reduced the usage efficient of lignocellulose but also decreased the property of the products made from liquefied wood. Therefore, it was helpful for solving practical problems to clarify the lignocellulosic liquefaction reaction mechanism. In past decades, Lin et al. (2001a, b, 2004), Yamada and Ono (2001) used the model compounds instead of natural lignin and cellulose in wood to study lignocellulosic liquefaction mechanism and finally obtained dozens or hundreds of the chemical structures of main decomposed products, meanwhile, illustrated that the liquefaction process was complicated considerably. Furthermore, to enrich basic research of lignocellulosic liquefaction, Kobayashi et al. (2004) studied the chemical structure and molecular weight of the liquefied wood residue in different liquefaction time by Fourier transform infrared (FT-IR) and Gel permeation chromatography (GPC). Pan et al. (2007), Zhang et al. (2006) and Yamada et al. (2001) investigated the yield of the liquefied wood residues by adding different charge ratio (liquefying reagents/lignocellulose, w/w) and changing the types of liquefying reagents in the liquefaction system. All the results showed the condensation reaction occurred in the last stage of lignocellulosic liquefaction and generated a large amount of condensated residue that was insoluble in organic solvents.

Based on the references, several possibilities about the formation reason of the condensation residue were reported. It might stem from the mutual reaction among small molecule from decomposition lignin or cellulose (Yamada et al. 2001, Zou et al. 2009, Chen et al. 2007, Hoess et al. 1988, Mocanu et al. 2010), and might due to the reaction between cellulose or lignin and liquefying reagents (Demirbas 2000). Because the lignocellulosic liquefaction process was inconstant, the research on condensation reaction has been insufficient and the formation reasons of the new condensed residues have not yet been ascertained until now.

Moreover, FT-IR and TG were used to analyze the chemical structure, thermal decomposition and pyrolysis mechanism of hemicellulose (Peng and Wu 2010), lignin (Wang et al. 2009, Liu et al. 2008) and organic materials (Court and Sephton 2009) in the previous researches, less researches on liquefied wood products were reported. Therefore, the goal of the research presented here was to study further the chemical groups variation and thermal behaviors in pyrolysis of liquefied wood products obtained in the initial stage such as 10, 25 and 60 minutes (decomposition products) and in the last stage of wood liquefaction such as 120, 150 and 180 minutes (condensation products) by FT-IR and TGA. By this work, some basic information can be provided to the study of wood liquefaction mechanism.

MATERIAL AND METHODS

Materials

Betula dahurica Pall wood was used for liquefaction material. Firstly, polyethylene glycol and glycerin (4/1, w/w) as the liquefying reagents and 72 % sulfuric acid as a catalyst were mixed with wood (polyhydric alcohols/wood/sulfuric acid, 3/2/0.03, w/w/w) to obtain the liquefied wood mixture at 150 °C. Then the mixture was diluted by acetone, and then filtered by glass-fiber filter paper (GA100, ADVANTEC, JAPAN) and the filtrates were used for the samples of FT-IR and TGA.

FT-IR measurement

A small amount of liquefied wood was directly analyzed by using a FT-IR spectrometer

(FT-IR 200, BRUKER, GERMANY). The scan times was 32, the distinguishability was 4 cm^{-1} and the scan range was 400cm^{-1} - 4000cm^{-1}.

TG measurement

The weight loss of wood and its liquefaction products were measured by thermogravimetry analyzer (DTG-60, SHIMADZU, JAPAN). First, 5-8 mg of the sample was placed in an Al_2O_3 ceramic pan. And then the samples were heated from 40 to 600 °C at the heating rate of 5, 10 and 20 °C.min^{-1}, respectively. At the same time, N_2 with a high purity was used as a carrier gas, and the flow rate of N_2 was 30 mL.min^{-1}.

RESULTS AND DISCUSSION

FR-IR analysis

Fig. 1 displays FT-IR spectra of wood and liquefied wood products in different liquefaction time.

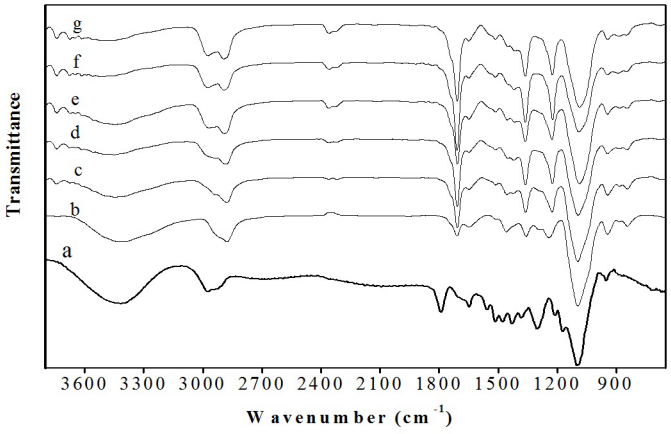

Fig. 1: FT-IR spectra of wood a) and liquefied wood products in b) 10, c) 25, d) 60, e) 120, f) 150 and g) 180 min. Liquefaction temperature, 150 °C; polyhydric alcohols/wood, 3/2, amount of sulfuric acid, 1 % (based on liquefying reagents)

The absorption peaks at 3364 cm^{-1} and 2923 cm^{-1} occurred in the spectra of wood and the liquefied wood products. A broad peak at around 3364 cm^{-1} was due to the –OH groups from either carbohydrates such as cellulose and hemicellulose or lignin. The peak at 2923 cm^{-1} represented the C-H stretch in methyl and methylene groups. The ketone and aldehyde groups at 1709 cm^{-1} from the polysaccharide compounds, and groups from the guaiacyl at 1243 cm^{-1} from the lignin (Pan et al. 2007) appeared also the aromatic rings at 1648 cm-1, the phenolic hydroxyl at 1357 cm^{-1}, the methoxy in the spectra of wood and liquefied wood products. It was suggested that the liquefied wood products retained still the basic structure units of lignin and cellulose even if condensation reaction occurred in the last stage of liquefaction. With the prolongation of liquefaction time, the intensity of absorption at 1709 cm^{-1} increased gradually,

which suggested the liquefaction time improved the extent of cellulose degradation; the intensity of the peak at 1648 cm^{-1} kept almost stable, which showed the liquefaction time had smaller effect on the aromatic ring of lignin; and the peaks at 1357 cm^{-1} and 1243 cm^{-1} became sharper, as was because lignin was further decomposed. The peak at 1250 cm^{-1} in wood spectra was shifted to 1243 cm^{-1} in the spectra of liquefied wood products. This shift might be caused by inductive effects of substituents in the aromatic ring system of lignin (Pastusiak 2003). In addition, the absorbance at 945 cm^{-1} was the polysaccharide group from cellulose (Faix 1991, Naumann et al. 1991), its number decreased litter by litter as a function of liquefaction time. It might be because these polysaccharide groups participated in the chemical reaction and generated insoluble compounds in the acetone solvent. To sum up, more functional groups from lignin could be observed on the spectra of liquefied wood products, especially for condensation products. Kobayashi et al. (2004) approved that the lignin could be completely degraded even in the initial stage of the liquefaction and converted to the soluble components. Thermal behaviors and kinetic parameters of liquefied wood products in TGA pyrolysis.

Weight loss percents at the three heating rates

Fig. 2 displays TG profiles of wood and the liquefied wood products in different liquefaction time at the three heating rates.

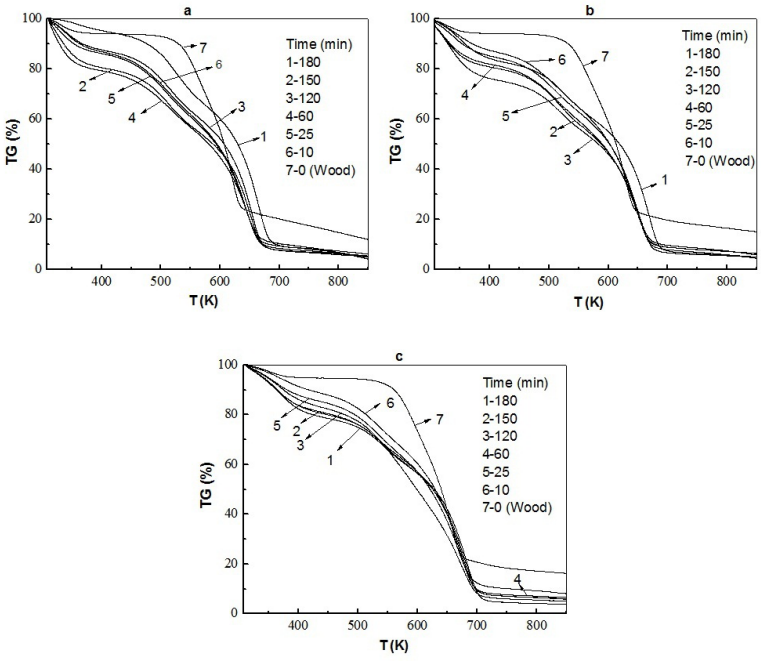

Fig. 2: TG profiles of wood and the liquefied wood products at the heating rates of a) 5, b) 10 and c) 20 °C.min^{-1}

The extent of the sample degraded in pyrolysis declined with the increase of heating rate in Fig. 2. And the TG profiles moved to higher temperature zone due to the increase of heating

rate under the condition of the same liquefaction time. It was suggested that pyrolysis at higher heating rate would need higher temperature to get the same weight loss. Wang and his coworkers (Wang et al. 2008) studied the pyrolysis of biomass and its three components under syngas and hydrogen and obtained the same results. Tab. 1 shows the weight loss percent and the residual ratios of all the samples at 20 $^{o}C.min^{-1}$.

Tab. 1: Weight loss percents and residual ratios in the main weight loss stages at 20$^{o}C.min^{-1}$

Liqu. time (min)	Temp. range (K), Weight loss percent (%)			Residual ratio (%)
	Stage 1	Stage 2	Stage 2	
0 (wood)	312-505 5.59	505-685 72.22		16.29
10	312-448 11.75	448-570 20.15	570-726 58.65	9.69
25	312-448 14.62	448-570 20.46	570-726 52.58	9.08
60	312-448 18.31	448-570 17.23	570-726 54.75	8.10
120	312-475 18.44	475-607 31.36	607-739 38.69	10.32
150	312-475 20.43	475-607 23.01	607-739 46.45	8.48
180	312-475 21.76	475-607 21.88	607-739 49.05	6.36

The main weight loss processes of all the liquefied wood products, different from that of wood itself, could be divided into three stages in Fig. 2. There were more differences in the TG profiles between wood and liquefied wood products. The weight loss percent of wood increased sharply at 500-650 K, while the weight loss processes of liquefied wood products were mainly in the range from 300 K to 700 K. The total weight loss percent of wood was less than those of liquefied wood products and the value was 77.81 %. The differences of the TG profiles from decomposition products and condensation products were smaller and the profiles were partly overlapped. The total weight loss ratios of the three stages of condensation products were higher than those of decomposition products and the residual ratios in pyrolysis were lower, which showed the thermal stabilities of the condensation products were worse and the condensation products were prone to participate in pyrolysis reaction. Furthermore, the residual ratio of condensation product in 180 minutes was lower than in 120 minutes, as illustrated that the liquefaction time could facilitate the degradation of condensation products and the condensation products with low molecular weight at 180 minutes had the worst thermal stability in all the samples.

Weight loss rate at the three heating rates

Fig. 3 illustrates the DTG profiles of wood and liquefied wood products at different heating rates.

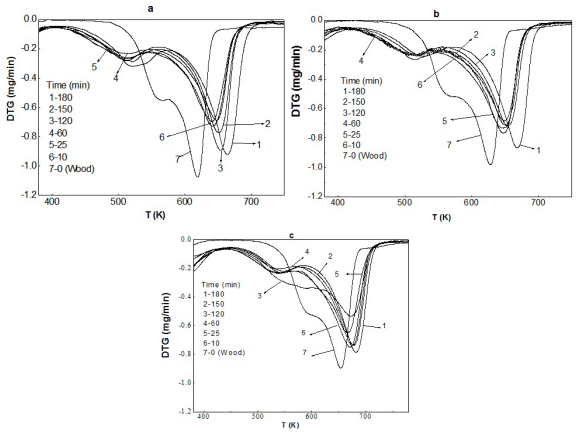

Fig. 3: DTG profiles of wood and liquefied wood products at a) 5, b) 10 and c) 20 °C.min^{-1}

The DTG profile of wood itself was different from those of liquefied wood products. The DTG peak of wood appeared at lower temperature zone, while the peaks of liquefied wood products distributed at higher temperature zone. DTG profile is a result of differential calculation for TG data, so the higher peak stands for higher weight loss rate. The difference of DTG profiles between wood and liquefied wood products indicated that the temperature at which weight loss rate was up to the maximum became higher after wood liquefaction. Furthermore, the curves moved gradually to the higher temperature zone with the increase of heating rate. This result was accordant with the influence of heating rate on TG profiles. The temperature and the height of the peak at 180 minutes were up to the maximums in all the liquefied wood products. The reason might be more chemical groups at 180 minutes improved reaction activity and accelerated reaction rate in TGA pyrolysis.

Heat at the three heating rates

The highest heating rate brought the sharpest peak and finally made the analysis of heat absorption more accurate, so the heating rate of 20 °C.min^{-1} was chosen as a parameter to get a series of differential thermal analysis (DTA) profiles. Fig. 4 displays DTA profiles of all the samples at 20 °C.min^{-1} under nitrogen.

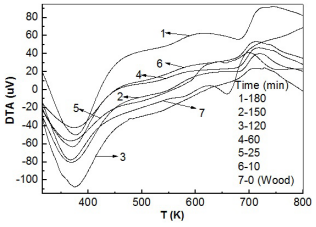

Fig. 4: DTA profiles of wood and liquefied wood products in the liquefaction time of wood (7), (6) 10, (5) 25, (4) 60, (3) 120, (2) 150 and (1) 180 min at 20 °C.min^{-1}

Two peaks occurred on the DTA profiles of all the samples. They all were endothermic peaks for wood, while for the liquefied wood products, one was an endothermic peak and the other

was an exothermic peak. In general, vitrifaction, liquation and decomposition can generate an endothermic peak; crystallization and oxidation can give an exothermic peak. The TGA pyrolysis reaction occurred at lower temperature and the oxidation might occur at higher temperature. The hydroxyl from liquefied wood products might be oxidized into aldehydes and carboxylic compounds. Moreover, the differences between decomposition products and condensation products on the DTA profiles were smaller. Tab. 2 shows endothermic and exothermic values of all the samples in the total pyrolysis stage at 20 °C.min^{-1}.

Tab. 2: Heat values of wood and liquefied wood products from different liquefaction time at 20 °C .min^{-1}

Liqu. time (min)	Peak temp. (K)		Heat	
	T_1	T_2	H_1 (kJ.g^{-1})	H_2 (J.g^{-1})
0 (Wood)	367.27	658.20	-2.60	-431.21
10	373.94	712.32	-1.15	382.21
25	367.39	698.21	-1.40	350.54
60	370.77	717.28	-1.19	670.30
120	374.66	728.14	-1.81	571.85
150	368.56	719.14	-1.30	309.89
180	376.50	744.60	-1.44	1130.00

For the endothermic peak, the heat absorption value of wood was the highest in all the samples and it was 2.60 J.g^{-1}. The result is possible because wood contained the cellulose component with more crystallize structure and these crystallize structure was difficult to be broken down in TGA pyrolysis. The heat value of 120 minutes was obviously higher than those of other liquefaction time and it was 1.81 kJ.g^{-1}. It was indicated that the thermal stability of the liquefied wood product of 120 minutes at 20 °C.min^{-1} was better, and it was hard to be degraded at high temperature. Furthermore, there were smaller differences in the heat value for other liquefied wood products. For the exothermic peak, the heat value of 180 minutes was the highest and it was 1130 J.g^{-1}, as might be a reason for the lowest residual ratio in TGA pyrolysis.

Non-isothermal thermogravimetric kinetics

Arrhenius equation is a basic equation of thermal analysis kinetics and it is expressed as the Equation (1):

$$\frac{d\alpha}{dt} = A\exp(-\frac{E}{RT})(1-\alpha)^n \quad (1)$$

where: ($d\alpha/dt$) is the conversion rate, n is reaction order that can be fraction and negative, A is apparent pre-exponential factor, R is the gas constant, E is the apparent activation energy, and α can be regarded as the conversion of the reactant at time t, which follows the Equation (2):

$$\alpha = \frac{W_0 - W_t}{W_0 - W_\infty} \quad (2)$$

where: W_0 is the initial mass before pyrolysis, W_t is the mass of the sample when reaction time is t, W_∞ stands for the residual mass of the sample after the reaction is completed.

Apparent activation energy and apparent pre-exponential factor

In the study on non-isothermal thermogravimetric kinetics, many methods can be used to calculate the apparent activation energy (E) and apparent pre-exponential factor (A). Kissinger (1957) Equation (3) was a common method.

$$\ln\left(\frac{\beta_i}{T_{pi}^{\ 2}}\right) = \ln\frac{AR}{E} - \frac{E}{R}\frac{1}{T_{pi}} \quad (i=1,2,\ldots,6) \tag{3}$$

where: β is the heating rate, T_p is the peak temperature on the DTA profile. According to this equation, linear function can be built by ln ($\beta.T_p^{-2}$) and $1.T_p^{-1}$. E values of all samples can be figured out through the slopes of the straight lines and A values can also be calculated by the intercepts of the straight line. Fig. 5 is the linear relationship between ln ($\beta.T_p^{-2}$) and $1.T_p^{-1}$ from liquefied wood products.

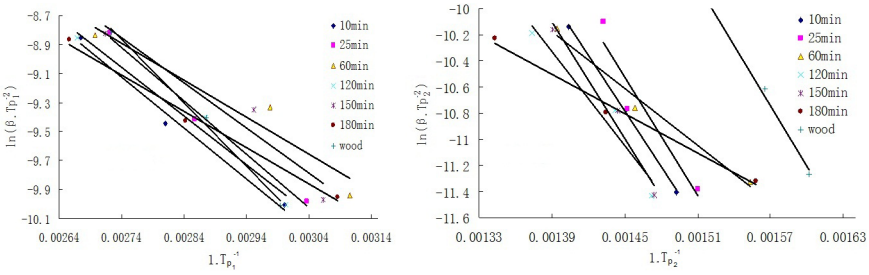

Fig.5: Linear relationships between ln ($\beta.T_p^{-2}{}_{(1,2)}$) and $1.T_p^{-1}{}_{(1,2)}$

Reaction order n

Simplified Crane (1972) Equation (4) is usually used to work out the reaction order n,

$$\ln\beta = -\frac{E}{nR}\times\frac{1}{T_P} + C \tag{4}$$

In this Equation, the reaction order n can be obtained by the linear relationship between Lnβ and $1.T_p^{-1}$. Fig. 6 displays the linear relationships between lnβ and $1.T_p^{-1}$ from liquefied wood products in different liquefaction time.

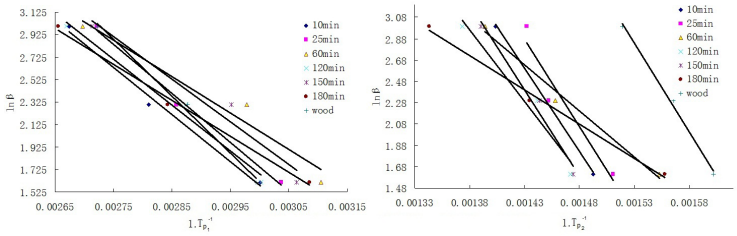

Fig. 6: Linear relationships between lnβ and $1.T_p^{-1}{}_{(1,2)}$

Tab. 3 shows the calculate results of apparent activation energy, apparent pre-exponential factor and reaction order at corresponding peak temperature in the Figs. 5 and 6.

Tab. 3: Kinetic parameters (E, A and n) values of all the samples

Liqu. time (min)	Heating rate (°C. min-1)	Peak temp. (K)		$E_1(R^2)$ (kJ.mol^{-1})	$E_1(R^2)$ (kJ.mol^{-1})	A1(s^{-1})	A2 (s^{-1})	n_1 (R^2)	n_2 (R^2)
		TP_1	TP_2						
0 (Wood)	5	334.05	624.35	36.05 (0.9921)	128.55 (0.9940)	103840	117×108	0.8623 (0.9944)	0.9234 (0.9950)
	10	347.73	638.75						
	20	367.27	658.20						
10	5	333.21	669.88	29.07 (0.9871)	117.84 (0.9976)	5499	2.49×108	0.8323 (0.9905)	0.9112 (0.9981)
	10	355.88	688.83						
	20	373.94	712.32						
25	5	329.34	662.06	30.65 (0.9917)	124.88 (0.9111)	12010	1.16×109	0.8415 (0.9937)	0.9171 (0.924)
	10	349.96	688.75						
	20	367.39	698.21						
60	5	322.04	643.84	21.22 (0.9278)	60.29 (0.9831)	382	6578.69	0.7865 (0.9555)	0.8424 (0.9874)
	10	335.86	685.81						
	20	370.77	717.28						
120	5	333.03	679.48	28.07 (0.974)	99.81 (0.9400)	4105	6.90×106	0.8267 (0.9828)	0.8950 (0.9517)
	10	347.93	693.61						
	20	374.66	728.14						
150	5	326.45	678.35	25.79 (0.9379)	122.88 (0.9710)	2174	5.04×108	0.8169 (0.9587)	0.9135 (0.9758)
	10	338.85	692.64						
	20	368.56	719.14						
180	5	324.06	641.91	20.86 (0.9915)	41.80 (0.9898)	269	149.81	0.7827 (0.9337)	0.7848 (0.9930)
	10	351.83	696.97						
	20	376.5	744.6						

Theoretically, apparent activation energy refers to the least energy of absorption or release when the samples are subject to the pyrolysis reaction. Its value is associated with the apparent pre-exponential factor by the Equation (3). The value will be generally higher when the apparent pre-exponential factor increases. The E_1 value range of all the samples was 20.86-36.05 kJ.mol^{-1} and the E_2 value was distributed in the range of 41.80-128.55 kJ.mol^{-1}. And the range of related coefficient corresponding to the E was respectively 0.9278-0.9921 and 0.9111-0.9976, which suggested that the linear fits of the E_s in the Fig. 5 were better.

The E values of wood were higher than those of the liquefied wood products. It was further indicated that the thermal stability of wood was better. In previous work (Niu et al. 2010), it was suggested that liquefaction residual yields of 25 minutes and 150 minutes were almost equal, which might was associated with the E values of 25 minutes and 150 minutes. In the Tab. 3, their apparent activation energy in the two liquefaction time was approximate. The liquefied wood product at 180 minutes had the smallest E value comparing with other products, as suggested that thermal stability of 180 minutes was the worst in all the samples.

Considering to the reaction order, the differences of all the samples were smaller, and the values were less than 1. The two reaction order of the samples was in 0.7827-0.8623 and 0.7848-0.9234 region, respectively. The range of related coefficient associated with the reaction order was respectively 0.9337-0.9944 and 0.924-0.9981, which suggested that the results of linear fits for the two reaction orders were better in Fig. 6. In a word, the results of the reaction

orders showed the liquefaction time had smaller effect on the TGA pyrolysis mechanism. The reasons for weight loss percent and heat variation in pyrolysis were mainly due to the differences of liquefied wood products themselves.

CONCLUSIONS

In this paper, FT-IR and TGA were used to analyze the function groups variation and thermal degradation behaviors of wood and liquefied wood products to understand completely the condensation reaction mechanism during wood liquefaction.

The results suggested that the number of function groups at 1709 cm^{-1} from cellulose and at 1648 cm^{-1}, 1357 cm^{-1} and 1243 cm^{-1} from lignin increased as a function of liquefaction time. Furthermore, with the increase of heating rate, the thermal stability of all the improved samples and the temperature at the highest weight loss rate rose. Compared with wood itself and the decomposition products, condensation products in the last stage of wood liquefaction were readily to be degraded in TGA pyrolysis and their thermal stability were worse.

For condensation products, the apparent activity energy was higher at 150 minutes and lower at 180 minutes. Judging by the reaction order, the liquefaction time had smaller effect on the TGA pyrolysis mechanism.

ACKNOWLEDGMENTS

This study was supported by Forestry Public Special Scientific Research in China (No. 201004057).

REFERENCES

1. Ahmadzadeh, A., Zakaria, S., 2009: Preparation of novolak resin by liquefaction of oil palm empty fruit bunches (EFB) and characterization of EFB residue. Polymer Plastics Technology and Engineering 48(1): 10-16.
2. Chen, F.G., Lu, Z.M., 2009: Liquefaction of wheat straw and preparation of rigid polyurethane foam from the liquefaction products. Journal of Applied Polymer Science 111(1): 508-516.
3. Chen, F.G., Xie, T., Lu, Z.M., 2007: Preparation and performances of modified epoxy resin from liquefied bagasse. Chemistry and Industry of Forest Products 27(03): 111-115.
4. Court, R.W., Sephton, M.A., 2009: Quantitative flash pyrolysis Fourier transform infrared spectroscopy of organic materials. Analytica Chimica ACTA 639(1-2): 62-66.
5. Crane, L.W., 1972: Analysis of curing kinetics in polymer composites. Journal of Polymer Science 12: 120-131.
6. Demirbas, A., 2000: Mechanisms of liquefaction and pyrolysis reactions of biomass. Energy Conversion & Management 41(6): 633-646.
7. Faix, O., 1991: Classification of lignin from different botanical origins by FT-IR spectroscopy. Holzforschung 45(Suppl.): 21-27.
8. Hoess, A., Arthur, A.K., Wanner, G., Fanning, E., 1988: Recovery of soluble, biologically active recombinant proteins from total bacterial lysates using ion exchange resin. Nature Biotechnology 6: 1214-1217.

9. Kissinger, H.E., 1957: Reaction kinetics in differential thermal analysis. Analytical Chemistry 29: 1702-1706.
10. Kobayashi, M., Asano, T., Kajiyama, M., Tomita, B., 2004: Analysis on residue formation during wood liquefaction with polyhydric alcohol. Journal of Wood Science 50(5): 407-414.
11. Kunaver, M., Jasiukaityte, E., Cuk, N., Guthrie, J.T., 2010: Liquefaction of wood, synthesis and characterization of liquefied wood polyester derivatives. Journal of Applied Polymer Science 115(3): 1265-1271.
12. Lin, L.Z., Yao, Y.G., Shiraishi, N., 2001a: Liquefaction mechanism of β-o-4 lignin model compound in the presence of phenol under acid catalysis. Part 1. Identification of the reaction products. Holzforschung 55(6): 617-624.
13. Lin, L.Z., Yao, Y.G., Shiraishi, N., 2001b: Liquefaction mechanism of β-o-4 lignin model compound in the presence of phenol under acid catalysis. Part 2. Reaction behavior and pathways. Holzforschung 55(6): 625-630.
14. Lin, L.Z., Yao, Y.G., Yoshioka, M., Shiraishi, N., 2004: Liquefaction mechanism of cellulose in the presence of phenol under acid catalysis. Carbohydrate Polymers 57(2): 123-129.
15. Liu, Q., Wang, S.R., Zheng, Y., 2008: Mechanism study of wood lignin pyrolysis by using TG-FTIR analysis. Journal of Analytical and Applied Pyrolysis 82(1): 170-177.
16. Mocanu, A.M., Odochian, L., Moldoveanu, C., Carja, G., 2010: TG-FTIR study on thermal degradation in air of some new diazoaminoderivatives (ii). Thermochimica ACTA 509(1-2): 33-39.
17. Naumann, D., Labischubski, H., Giesbrecht, P., 1991: The characterization of microorganisms by Fourier transform infrared spectroscopy (FTIR). In: Nelson WH(ed) Modern Techniques for rapid microbiological analysis. VCH, New York. Pp 43–96.
18. Niu, M., Zhao, G.J., Alma, M.H., 2010: Molecular mechanism of condensation reaction during wood liquefaction with polyhydric alcohols-chemical groups, crystallinity and microcosmic morphological characteristics of the residues. Journal of Beijing Forestry University.
19. Pan, H., Shupe, T.F., Hse, C.Y., 2007: Characterization of liquefied wood residues from different liquefaction conditions. Journal of Applied Polymer Science 105(6): 3739-3746.
20. Pastusiak, R., 2003: Charakterisierung von Zellstoffkomponenten-Analytik, Spektroskopie, Reaktions kinetik und Modellierung. Dissertation, Fakultät für Chemie der Technischen Universität München.
21. Peng, Y.Y., Wu, S.B., 2010: The structural and thermal characteristics of wheat straw hemicellulose. Journal of Analytical and Applied Pyrolysis 88(2): 134-139.
22. Vázquez, G., Antorrena, G., González, J., Freire, S., 1997: FTIR, ^{1}H and ^{13}C NMR characterization of acetosolv-solubilized pine and eucalyptus lignins. Holzforschung 51(2): 158-166.
23. Wang, G., Li, W., Li, B.Q., Chen, H.K., 2008: TG study on pyrolysis of biomass and its three components under syngas. Fuel 87(4-5): 552-558.
24. Yamada, T., Hu, Y., Ono, H., 2001: Condensation reaction of degraded lignocellulose during wood liquefaction in the presence of polyhydric alcohols. Journal of Adhesion Society of Japan 37(12): 471-478.
25. Yamada, T., Ono, H., 2001: Characterization of the products resulting from ethylene glycol liquefaction of cellulose. Journal of Wood Science 47(6): 458-464.
26. Zhang, Y.C., Ikeda, A., Hori, N., Takemura, A., Ono, H., Yamada, T., 2006: Characterization of liquefied product from cellulose with phenol in the presence of sulfuric acid. Bioresource Technology 97(2): 313-321.

27. Zou, X.W., Yang, Z., Qin, T.F., 2009: FTIR analysis of products derived from wood liquefaction with 1-Octanol. Spectroscopy and Spectral Analysis 29(6): 1545-1548.

Min Niu, Guangjie Zhao
Beijing Forestry University
College of Materials Science & Technology
Qinghua Eastroad 35
Haidian
Beijing
China 100083
Corresponding author: niumin521@163.com

Mehmet Hakki Alma
Kahramanmaras Sutcu Imam University
Faculty of Forestry
Kahramanmaras
Turkey 46100